Nonlinear Microwave Signal Processing in Yttrium-Iron Garnet (YIG) Films

Gennadiy Melkov*, Yurij Kobljanskyj*, Alexander Serga*, Vasil Tiberkevich*, and Andrei Slavin**

Abstract **– A nonlinear microwave signal processor based on the parametric interaction of a microwave magnetostatic wave, propagating in an yttrium-iron garnet (YIG) film waveguide, with a non-stationary (pulsed) electromagnetic pumping is proposed and practically realized. The proposed processor amplifies input pulsed microwave signals by up to 30 dB, performs operations of phase conjugation, time profile inversion, and controlled time delay of up to 1 μs.**

1. Introduction

Dipolar spin waves or magnetostatic waves (MSW) (see chapter 6 in [1]), propagating in magnetized to saturation yttrium–iron garnet (YIG) films, can be used for processing of microwave electromagnetic signals in a way similar to that of surface acoustic waves (SAW) [2], propagating in LiNb or other acoustic crystals. The important advantage of microwave signal processors based on MSW is a much higher working frequencies which can easily reach 10 GHz, while the working frequencies of SAW devices rarely exceed 2 GHz [2].

The proposed nonlinear MSW signal processor is based on a conventional MSW delay-line structure [3-7], consisting of an YIG film waveguide tangentially magnetized by the external bias field H_0, input transducer situated at one end of the film waveguide, and the output transducer situated at the other end. The input transducer converts the input electromagnetic signal into a relatively slow magnetostatic wave (typical group velocity $v \sim 10^6$ cm/sec), which propagates in the film towards the output transducer, where it is again converted into the electromagnetic wave. The delay time in such a structure depends on the thickness of the YIG film, distance between the transducers, and the magnitude of the bias magnetic field H_0, and varies from several tens to several hundreds of nanoseconds.

Magnetostatic waves propagating in YIG films are dispersive and, for sufficiently large powers of the input signal ($P_{\text{in}} \sim$ several mW), are also nonlinear. Nonlinear and dispersive properties of MSW in YIG films allow us to perform several useful operations on the microwave signal during its presence in the film in the form of an MSW pulse, such as: pulse compression and formation of envelope solitons [5], amplification [6], wave front reversal and phase conjugation [7], etc. Detailed theoretical analysis of these effects is given in our papers [6, 7].

In our current paper we describe the action of a MSW signal processor in the case when an additional pumping electromagnetic pulsed field (having frequency ω_p, which is approximately two times larger than the carrier frequency of the input microwave signal $\omega_p \approx 2\omega_s$) was supplied to the YIG film. The magnetic field $\mathbf{h}_p$ of the pumping pulse was directed mostly parallel to the bias magnetic field $\mathbf{H}_0$, so that the situation of parametric *parallell pumping* (see chaper 10 in [1] and [8]) was realized in the film. Under these circumstances, the three-wave first-order parametric interaction process between the propagating MSW signal and the localized pumping magnetic field was happening in the film. As a result of this process, the signal MSW, propagating towards the output tranducer, was parametrically amplified, and a reversed and phase conjugated ("idle") MSW, having frequency $\omega_i = \omega_p - \omega_s$ and propagating from the region of pumping localization towards the input tranducer, was parametrically excited [7].

2. Constructions of MSW Processors

The schematic view of type 1 of the studied MSW processors is shown in Fig. 1. The input (1) and output (2) transducers were short-circuited microstrip lines of the width 50 μm, and were separated by the distance $l = 5$ mm. A tangentially magnetized (bias magnetic field $H_0 = 1020$ Oe) YIG film waveguide (in-plane sizes of 1.6 mm x 18 mm, thickness of 4.9 μm, saturation magnetization $4\pi M_0 = 1750$ Oe, ferromagnetic resonance linewidth measured at 5 GHz $2\Delta H = 0.4$ Oe) was placed on top of the delay-line structure. The input signal pulses of varying duration 15 ns < τ_s < 50 ns and power $0 < P_{\text{in}} < 3$ W were supplied to the input transducer. The carrier frequency ω_s of input pulse was chosen to be $\omega_s/2\pi = 4720$ MHz, which corresponds to the carrier wave number of $k_s = 155$ cm^{-1} and group velocity

* National Taras Shevchenko University of Kiev, Radiophysical Faculty, 64 Volodymyrs'ka Str., Kiev 01033, Ukraine. E-mail: mga@boy.rpd.univ.kiev.ua, Tel: +380-44-2660532, Fax: +380-44-2660600.
** Oakland University, Department of Physics, Rochester, Michigan 48309-4487, USA. E-mail: slavin@oakland.edu, Tel: +1-248-3703401, Fax: +1-248-3703408.

v = -2.21 cm/μs (backward volume magnetostatic waves or BVMSW were used [9]).

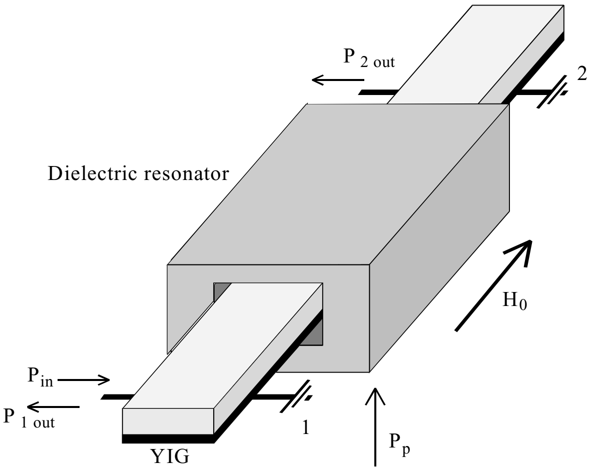

Figure 1: Type 1 MSW processor. P_{in} and $P_{2\ out}$ – input and output powers at the signal frequency ω_s, respectively; $P_{1\ out}$ – output power at the idle frequency $\omega_i = \omega_p - \omega_s$; P_p – pumping power applied to the dielectric resonator.

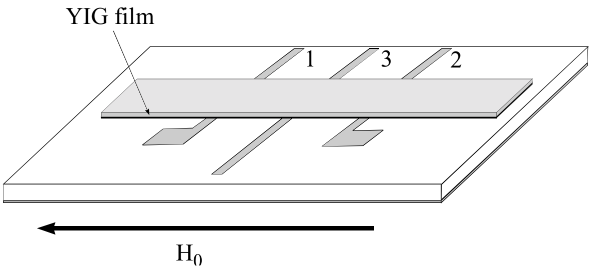

Figure 2: Type 2 MSW processor. 1, 2, and 3 – input, output, and pumping microstrip transducers, respectively.

To create a spatially extended region of parallel pumping localization (L = 3.3 mm in our experiment) the pumping pulse was supplied to an open dielectric resonator situated between the microstrip transducers and made of a thermostable ceramics (dielectric permeability $\varepsilon \approx 80$). The central part of the ferromagnetic film was inside the dielectric resonator (see Fig. 1). The carrier frequency of the pumping pulse was chosen to be $\omega_p = 2\omega_s = 2\pi \cdot 9440$ MHz, the maximum pumping power was $P_{p\ max}$ =5 W, and the pumping pulse duration was varied in the interval 4 ns < τ_p < 150 ns.

The type2 MSW processor (Fig. 2) was almost the same as first one, except for the pumping dielectric resonator which was replaced by the microstrip resonator (3) of the width W = 50 μm, situated in the middle of the film between the input (1) and output (2) transducers. Electromagnetic pumping field was localized in the region of the width L = 220 μm around the pumping transducer. The YIG film thickness in this case was chosen to be 30.3 μm.

3. Experimental Results

3.1. Amplification and Phase Conjugation

Fig. 3 shows the experimentally measured and theoretically calculated (using the theory [6]) curves of the amplification factor for the transmitted signal ($K_{2\ out} = P_{2\ out}/P_{in}$) and conversion factor for the reversed and phase conjugated signal ($K_{1\ out} = P_{1\ out}/P_{in}$) *vs.* the pumping power P_p for different values of the pumping pulse duration τ_p in the type 1 MSW processor (Fig. 1). As it is clear from Fig. 3, the MSW processor Fig. 1 demonstrates a sufficiently large (exceeding 30 dB) parametric amplification of the input microwave pulsed signals.

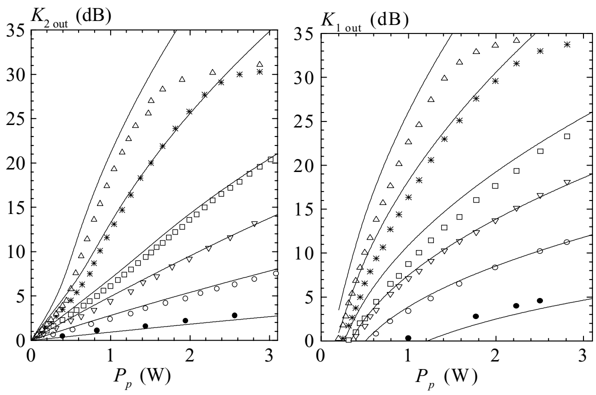

Figure 3: Amplification $K_{2\ out}$ and conversion $K_{1\ out}$ factors of the input signal *vs.* pumping power P_p for different values of the pumping pulse duration τ_p: ● – 10 ns, ○ – 20 ns, ∇ – 30 ns, □ – 40 ns, * – 60 ns, Δ – 80 ns. Solid lines – theoretical calculations using [6].

3.2 Inversion of the Time Profile

The experiments done on the type 1 MSW processor (Fig. 1) have shown, that, under certain conditions, the reversed and phase-conjugated ("idle") signal ($P_{1\ out}$ in Fig. 1) could have a time profile, that is *inverted* in respect to the time profile of the input signal [4]. To achieve this effect, it is necessary to have a weakly localized and non-stationary pumping, so that the length of the pumping localization region L is larger, than the length of the input pulsed signal $L > v\tau_s$, and the duration of the pumping pulse τ_p is much smaller than the duration of the input pulsed signal τ_s ($\tau_p << \tau_s$). To investigate the phenomenon of inversion of the input signal time profile, we used input signals in the form of two-pulse sequences with different amplitudes of the first and second pulse. The results of these experiments are presented in Fig. 4. It is clear, that the time profile of the reversed signal (pulses 2′ and 1′) is inverted in respect to the time profile of the input signal (pulses 1 and 2).

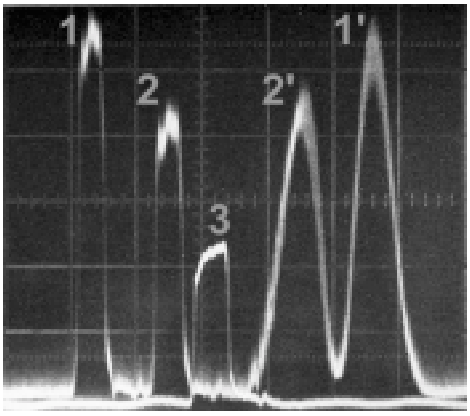

Figure 4: The experimental results of the time profile inversion for the two-pulse asymmetric input signals: 1, 2 – pulses in the input signal, 1′, 2′ – pulses in the reversed signal, 3 – pumping pulse.

3.3 Controlled Time Delay

As it was mentioned above, usually the time delays in MSW delay lines do not exceed several tenths of a microsecond. The type 2 active MSW processor with external parametric pumping (see Fig. 2) could increase these delay times by more than one order of magnitude. This function of the active MSW processor Fig. 2 is based on the effect of *spin wave momentum relaxation reversal* discovered in [10].

It was found experimentally in [10], that when in the structure Fig. 2 a pumping pulse was supplied to the middle transucer *later* then the input pulse passed this transducer, an *additional* amplified pulse (besides the usual delayed and attenuated signal pulse) appeared at the output transducer. We believe, that this additional pulse results from the parametrically amplified by pumping short and slow spin waves, that were formed in the process of *linear two-magnon scattering* of the original signal pulse on defects and inhomogeneities in the YIG film (chapter 11 in[1] and [11]).

This two-magnon scattering of the propagating signal wave takes place in all real magnetics and gives the main contribution to the observed linewidth of non-homogeneous magnetostatic precession modes and long-wave ($k_s \leq 10^2$ cm^{-1}) dipolar spin waves (magnetostatic waves) in magnetic crystals (chapter 11 in [1]). As a result of the two-magnon scattering, the original (signal) MSW, having wavevector $\mathbf{k}_s$, excites relatively short spin waves having wave vectors $\mathbf{k}$ with magnitudes $k \approx | k_s \pm 2\pi/a |$, where $a \sim 1$ μm is the size of the defect which caused scattering. These short secondary spin waves, created in the scattering process, have low group velocities ($v_\mathbf{k} << v$) (chapter 7 in [1]). Therefore, these secondary spin waves remain near the defect and can interact with it during a relatively long time interval after the signal wave had passed the defect and left the scattering region.

The interaction of a signal wave with defects is usually linear and reciprocal. Thus, the short secondary spin wave with the wave vector $\mathbf{k}$, localized near the defect and oscillating with its eigen-frequency $\omega_\mathbf{k}$ (which is not exactly equal to the signal frequency ω_s), can interact again with the defect, and generate an additional wave with the wave vector $\mathbf{k}_s$. However, since the amplitudes of these secondary spin waves are small and their frequencies and phases are random, the amplitude of the additional signal in the absence of pumping does not exceed the noise level. On the other hand, the presence of parametric pumping leads to the selective amplification of secondary spin waves having frequencies $\omega_\mathbf{k} \approx \omega_p/2$ [8] and, as a result, to the appearance of the additional macroscopic signal, that can be easily detected at the output transducer of the MSW processor. The amplitude and the time delay t_{12} of this additional pulse relative to the usual output pulse (see the inset in Fig. 5) depends on the pumping pulse power P_p and the moment of time when this pumping pulse was supplied to the middle transducer.

In our experiments on the type 2 MSW prosessor (Fig. 2) a rectangular microwave signal pulse of the carrier frequency $\omega_s = 2\pi{\cdot}4.7$ GHz, duration $\tau_s = 50$ ns, and power $P_{\text{in}} = 5$ mW was supplied to the input transducer, and was propagating with group velocity $v = 13$ cm/μs in the YIG film sample (film thickness $d = 30.3$ μm, distance between the input and output transducers $l = 5$ mm). The delay time of the signal $\tau_d = l/v$ was 38 ns. In the process of propagation the signal pulse was scattered on the defects and inhomogeneities in the film. The pumping pulse of the carrier frequency $\omega_p = 2\omega_s = 2\pi{\cdot}9.4$ GHz, duration $\tau_p = 150$ ns, and power $P_p = 5$ W was supplied to the pumping transducer (3) (see Fig. 2). The pumping was switched on Δt ns *after* the trailing edge of the signal pulse left the region of pumping localization. Microwave pumping magnetic field was created only in the immediate vicinity of the pumping transducer, so the direct interaction of the signal and pumping was excluded.

The results of our experiments are presented in Fig. 5. The inset in Fig. 5 shows the oscillogram of the signal at the output transducer. It can be seen, that besides the usual delayed and attenuated signal pulse (1), an additional amplified and further delayed pulse (2) was observed. The magnitude and the time delay of this second pulse (2) are strongly dependent on the parameters of the pumping pulse. We would like to stress, that this additional pulse (2) is observed at the output *only* if the primary signal pulse (1) had passed in the film *before* the pumping has been switched on. *The pumping alone does not generate this pulse*.

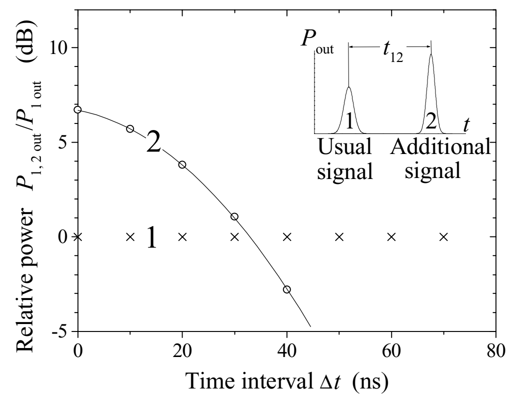

Figure 5: Dependence of peak powers of the usual (1) and additional (2) output signals on the time interval Δt between the signal and pumping pulses at the pumping transducer: symbols – experiment, solid line – theoretical calculation using [10]. Inset shows schematic view of the signals received at the output transducer.

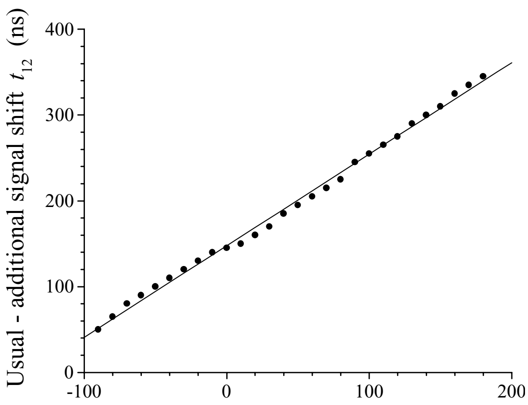

Figure 6: Dependence of the time delay t_{12} of the additional output pulse (pulse (2) in Fig. 5) on the time interval Δt between the signal and pumping pulses at the pumping transducer.

It is clear from the inset in Fig. 5, that the additional output pulse (2) is delayed relative to the usual output signal (1) by the time t_{12}. The dependence of this time delay on the time interval Δt between the moment when the usual signal left the pumping transducer and the moment when the pumping pulse was switched on is shown in Fig. 6. It can be seen, that the time delay t_{12} of the additional pulse is directly proportional to the time interval Δt, and reaches the value of 340 ns, which is almost 9 times larger than the time delay (τ_d = 38 ns) of the usual signal in the same delay line structure. The maximum delay time of the additional pulse obtained in our experements exceeded 1 μs.

4 Conclusions

In conclusion, we have developed an active nonlinear microwave signal processor based on MSW propagating in a YIG film, and interacting with localized and pulsed electromagnetic pumping field. The developed processor, working at the signal carrier frequency of 4.7 GHz, demonstrated the signal amplification gain of 30 dB, controlled time delay of up to 1 μs, and allowed us to obtain the inversion of the time profile of the input pulsed signal.

This work was supported by the NSF grant DMR-0072017, and by the CRDF grant UP1-2120.

References

[1] A. G. Gurevich and G. A. Melkov, Magnetization Oscillations and Waves, CRC Press, N. Y., 1996.

[2] W. S. Ishak, Proc. IEEE, vol. 76, 1988, p. 171.

[3] A. V. Bagada, G. A. Melkov, A. A. Serga, and A. N. Slavin, Phys.Rev.Lett. vol.79, 1997, p. 2137.

[4] G. A. Melkov *et al.*, Phys. Rev. Lett., vol. 84, 2000, p. 3438.

[5] M. Chen, M. A. Tsankov, J. M. Nash, and C. E. Patton, Phys.Rev. B, vol. 49, 1994, p. 12773.

[6] G. A. Melkov *et al.*, JETP, vol. 89, 1999, p. 1189.

[7] A. L. Gordon *et al.*, JETP Lett., vol. 67, 1998, p. 913.

[8] V. S. L'vov, Wave Turbulence Under Parametric Excitation, Springer, Berlin-Heidelberg, 1994.

[9] R. W. Damon and J. R. Eshbach, J. Phys. Chem. Solids, vol. 19, 1961, p. 308.

[10] G. A. Melkov, Yu. V. Kobljanskyj, A. A. Serga, V. S. Tiberkevich, and A. N. Slavin, "Reversal of Momentum Relaxation", Submitted to Phys. Rev. Lett., January 2001.

[11] M. Sparks, Ferromagnetic Relaxation Theory, McGraw-Hill, N. Y., 1964.